

In J.-F. Aujol, M. Nikolova, N. Papadakis (Eds.):  
Scale Space and Variational Methods in Computer Vision.  
Lecture Notes in Computer Science, Vol. 9087, pp. 425–436, Springer, Berlin, 2015.  
The final publication is available at [link.springer.com](http://link.springer.com).

# Variational Exposure Fusion with Optimal Local Contrast

David Hafner and Joachim Weickert

Mathematical Image Analysis Group,  
Faculty of Mathematics and Computer Science,  
Campus E1.7, Saarland University, 66041 Saarbrücken, Germany  
`{hafner,weickert}@mia.uni-saarland.de`

**Abstract.** In this paper, we present a variational method for exposure fusion. In particular, we combine differently exposed images to a single composite that offers optimal exposedness, saturation, and local contrast. To this end, we formulate the output image as a convex combination of the input, and design an energy functional that implements important perceptually inspired concepts from contrast enhancement such as a local and nonlinear response. Several experiments demonstrate the quality of our technique and show improvements w.r.t. state-of-the-art methods.

**Keywords:** Exposure fusion, variational method, contrast enhancement

## 1 Introduction

Classical high dynamic range (HDR) methods combine several low dynamic range (LDR) images to one HDR image with the help of the exposure times and the camera response function [21, 15]. However, displaying these HDR results on standard monitors or printing them requires to compress the high dynamic range again. This process is called *tone mapping* [28]. If the main focus lies on such a displayable, well-exposed LDR image and the HDR composite is just seen as a necessary byproduct, the so-called *exposure fusion* technique is an interesting alternative [23]. In contrast to the described two-step procedure, the task here is to directly fuse the differently exposed images to an overall well-exposed composite. Such an exposure fusion approach has several advantages: First, there is no need to know the exposure times or the camera response function. Second, this one-step approach allows a direct tuning of the final results without the need of an intermediate HDR reconstruction. Most existing exposure fusion methods pursue the following processing pipeline: Based on some defined well-exposedness measures, weighting maps are determined for each of the input images. With these weighting maps all images are fused to the final composite.

*Our Contributions.* In contrast to those methods, our main idea is not to select the best input image parts in a first step and to combine them to one image afterwards. Instead, we directly formulate an energy whose minimiser gives the optimal result. More specifically, we do not compute the weighting maps just by considering features of the input images. Rather, we determine them in a result-driven fashion, i.e. in such a way that the fused image shows the best quality in terms of our model assumptions. We base our model on fundamental findings in histogram modification and contrast enhancement with differential equations [29, 7, 24], and formulate it in a transparent variational framework. This results in a mathematically well-founded method that yields better quality than state-of-the-art approaches, e.g. in terms of perceived local contrast.

*Outline.* We start with a discussion of related work in Section 2. After that, we present our variational approach for exposure fusion in Section 3. Its minimisation (Section 4) gives the desired fused image. The experiments in Section 5 demonstrate the quality of our method. We conclude with a summary and outlook in Section 6.

## 2 Related Work

Most previous exposure fusion approaches have the following workflow: In a first step they determine, based on specific quality measures, for each pixel or region of the input images how much it should contribute to the final composite. Such quality measures are for instance the magnitude of the Laplacian [10, 23], the textureiness [27], the entropy [17, 18], or the colour saturation [23, 32, 33]. In a second step, these pixels or regions are fused to the resulting overall well-exposed image. Here, the fusion strategies vary from region-based blending [17, 35] and pixelwise weighted averaging [27, 18, 32, 31, 33] to gradient domain fusion [13, 34] and pyramid-based techniques [12, 10, 23].

In contrast to all these approaches, we do not specify the quality of the input images first and then fuse them later on. Instead, we directly design the quality of the fusion result. In this regard, Raman and Chaudhuri [26] formulate an energy functional whose minimiser gives the fused composite. However, optimising the energy immediately for the image itself has several drawbacks: First, it restricts the possible model assumptions. Second and even more severely, it requires to impose a smoothness constraint on the resulting image. This is not intuitive and may lead to over-smoothed results. A more suitable idea of Kotwal and Chaudhuri [19] is to express the composite image as a weighted average of the input images and to optimise for these weights. This still allows to directly model assumptions on the fusion result, but additionally opens the possibility to impose a smoothness constraint on the weight maps and not on the image itself.

We follow this idea and incorporate perceptually inspired model assumptions that allow superior results. To formulate these assumptions by a suitable energy functional, we make use of important findings in variational histogram modification and contrast enhancement. Based on the seminal work of Sapiro and

Caselles [29], Bertalmío et al. [7] introduce a variational approach to locally increase the contrast of an image. In this context, Palma-Amestoy et al. [24] investigate several perceptually inspired energy terms. In his recent study, Bertalmío [6] shows connections to visual neuroscience.

These contrast enhancement approaches have found first applications in an exposure fusion related context: In their two-stage tone mapping operator, Ferradans et al. [16] apply a variational contrast enhancement in the second stage. Moreover, Bertalmío et al. [8] propose an energy-based method to fuse two differently exposed images. The fused result includes the details of the short exposure, and the colours are intended to resemble them of the long exposure. Piella [25] incorporates a gradient domain term in the energy of [7]. This forces the similarity to a precomputed gradient field that combines the gradients from multiple images. The success of these approaches motivates us to also base our model on those perceptually inspired contrast enhancement concepts. Along this line, we present in this paper a variational exposure fusion technique that handles multiple input images and is tailored to static scenes.

### 3 Energy Formulation

Our goal is to fuse  $n$  differently exposed images  $f_1, \dots, f_n$  to a single composite that is well-exposed everywhere and shows a visually pleasant local contrast. Basically, we propose to compute the fused image  $u$  as a pixelwise weighted average:

$$u(\mathbf{x}) = \sum_{i=1}^n w_i(\mathbf{x}) \cdot f_i(\mathbf{x}), \quad (1)$$

where  $\mathbf{x} = (x_1, x_2)^\top$  denotes the position on the rectangular image domain  $\Omega \in \mathbb{R}^2$  and  $w_i$  the weight of the input image  $i$ . We constrain these weights to be non-negative and to sum up to 1, i.e.  $w_i(\mathbf{x}) \geq 0$  and  $\sum_{i=1}^n w_i(\mathbf{x}) = 1$ . This provides a close attachment to the input data that prevents undesirable effects such as colour shifts or halos.

Most previous research concentrates on defining the image weights  $w_1, \dots, w_n$  based on the quality of the *input*. In contrast, we compute optimal weight maps for fusing an *output* image that features important perceptual properties such as a high local contrast. More specifically, they are optimal in the sense that the resulting composite  $u$  is optimal for the following energy functional:

$$\begin{aligned} E(w_1, \dots, w_n) = & \frac{1}{2} \int_{\Omega} \left( (u(\mathbf{x}) - \mu)^2 + (u(\mathbf{x}) - \bar{f}(\mathbf{x}))^2 \right) d\mathbf{x} \\ & - \frac{\gamma}{2} \int_{\Omega} \int_{\Omega} g_{\sigma}(\mathbf{x}, \mathbf{y}) \cdot \Psi_{\lambda}(u(\mathbf{x}) - u(\mathbf{y})) d\mathbf{x} d\mathbf{y} \\ & + \frac{\alpha}{2} \int_{\Omega} \sum_{i=1}^n |\nabla w_i(\mathbf{x})|^2 d\mathbf{x} \end{aligned} \quad (2)$$

subject to

$$w_i(\mathbf{x}) \geq 0 \quad \text{and} \quad \sum_{i=1}^n w_i(\mathbf{x}) = 1, \quad (3)$$

where the dependency of  $w_1, \dots, w_n$  from  $u$  is given by (1).

Let us examine the components of the presented energy step by step:

*Dispersion Term.* Following Bertalmío et al. [7], we model a so-called dispersion term in the first line of (2): The first part of this dispersion term favours solutions with an average grey value close to  $\mu$ , which is in general set to  $1/2$  for grey values in the range of 0 and 1. This implements the grey world principle [11, 24] and provides well-exposed images. The second part forces a similarity of  $u$  to the attachment image  $\bar{f}$ , which we determine by an average over all input images. As discussed in [24], this provides an attachment to the original data and accounts for the colour constancy assumption [20].

*Contrast Term.* The second term, the contrast term, counteracts this dispersion term, since it penalises uniform images much more than images with a high local contrast. Intuitively speaking, the energy favours solutions that differ a lot from pixel to pixel. Please note the minus sign in front of the contrast term. Here, the locality is introduced by the Gaussian weighting  $g_\sigma(\mathbf{x}, \mathbf{y}) := \frac{1}{2\pi\sigma^2} \exp\left(\frac{-|\mathbf{x}-\mathbf{y}|^2}{2\sigma^2}\right)$ . Furthermore,  $\Psi_\lambda(s) := \sqrt{s^2 + \lambda^2}$  is a function with a sigmoid-shaped derivative that shows connections to the nonlinear response of the visual system [22, 24]. The parameter  $\lambda$  allows to tune this nonlinear behaviour, and  $\gamma \geq 0$  weights the influence of the contrast term.

*Regularisation Term.* The third term in our energy functional is a regularisation term that rewards smooth weight maps. It renders the assumption that neighbouring pixels in the fused composite should have similar weights. Here  $\nabla := (\partial_{x_1}, \partial_{x_2})^\top$  denotes the spatial gradient operator, and  $\alpha \geq 0$  steers the amount of smoothness.

*Simplex Constraint.* Last but not least, the simplex constraint (3) restricts the fusion result to (pixelwise) convex combinations of the input images. Hence, it provides an additional natural attachment to the input data.

*Adaptation to Colour Images.* In the case of colour images, we compute joint weight maps for all channels. To this end, we transform the input images from the RGB to the YCbCr colour space and define  $u$  in (2) as the Y channel. Moreover, saturated colours make images to look vivid and expressive. Hence, we extend our energy (2) with the following *saturation term*:

$$-\frac{\beta}{2} \int_{\Omega} \left( (u_{Cb}(\mathbf{x}) - 1/2)^2 + (u_{Cr}(\mathbf{x}) - 1/2)^2 \right) d\mathbf{x}, \quad (4)$$

---

**Algorithm 1:** Projection onto simplex [30].

---

**Input:** weights  $w_1, \dots, w_n$

**Output:** projected weights  $\tilde{w}_1, \dots, \tilde{w}_n$

- 1  $\mathbf{s} = \text{sort}(w_1, \dots, w_n)$  such that  $s_1 \geq \dots \geq s_n$
  - 2  $m = \max \left\{ j \in \{1, \dots, n\} \mid s_j - \frac{1}{j} \left( \sum_{i=1}^j s_i - 1 \right) > 0 \right\}$
  - 3  $\theta = \frac{1}{m} \left( \sum_{i=1}^m s_i - 1 \right)$
  - 4  $\tilde{w}_i = \max \{ w_i - \theta, 0 \}$
- 

where  $u_{Cb}$  and  $u_{Cr}$  denote the Cb and Cr channels of  $u$ , respectively. This term favours values different from grey, and thus fused images with vivid colours. Here, the positive parameter  $\beta$  allows to control the amount of colour saturation. Once again, the minus sign should be noted.

## 4 Minimisation

To minimise energy (2) with the simplex constraint (3), we apply a projected gradient method; see e.g. Bertsekas [9]. Basically, each iteration consists of (i) a gradient descent step, followed by (ii) a projection onto the simplex.

*Gradient Descent.* With iteration index  $k$  and time step size  $\tau$ , the gradient descent of the energy functional (2) with the saturation term (4) reads

$$\begin{aligned}
 w_i^{k+1}(\mathbf{x}) = & w_i^k(\mathbf{x}) - \tau \cdot \left( f_{Y_i}(\mathbf{x}) \left( 2u_Y^k(\mathbf{x}) - \mu - \bar{f}_Y(\mathbf{x}) \right. \right. \\
 & \left. \left. - \gamma \int_{\Omega} g_{\sigma}(\mathbf{x}, \mathbf{y}) \cdot \Psi'_{\lambda}(u_Y^k(\mathbf{x}) - u_Y^k(\mathbf{y})) \, d\mathbf{y} \right) \right. \\
 & \left. - \beta \left( f_{Cb_i}(\mathbf{x}) (u_{Cb}^k - 1/2) + f_{Cr_i}(\mathbf{x}) (u_{Cr}^k - 1/2) \right) \right. \\
 & \left. - \alpha \Delta w_i^k(\mathbf{x}) \right), \tag{5}
 \end{aligned}$$

for  $i=1, \dots, n$  and  $(u_Y^k, u_{Cb}^k, u_{Cr}^k)^{\top} = \sum_{i=1}^n w_i^k(\mathbf{x}) \cdot (f_{Y_i}, f_{Cb_i}, f_{Cr_i})^{\top}$ . We discretise this equation with finite differences on a rectangular grid, and approximate the integral with the rectangle method.

*Projection onto Simplex.* After each gradient descent step, we account for the constraint (3) by projecting the computed weights onto the  $n$ -dimensional simplex; see Algorithm 1.

We assume the complete algorithm to be converged if the root mean square difference of two fusion results between 100 iterations is less than  $10^{-4}$ .

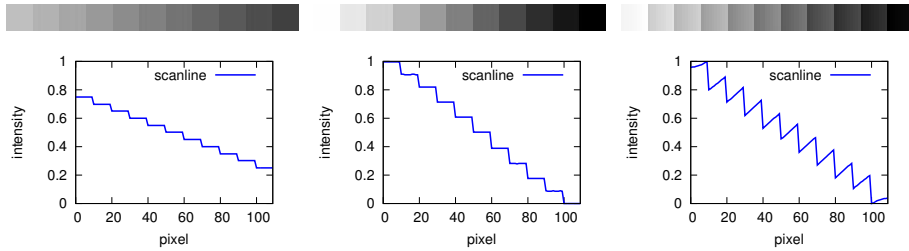


**Fig. 1.** Global vs. local contrast term for histogram equalisation. *From left to right:* Input, with global contrast term, with local contrast term. *Top:* Intensity images. *Bottom:* Corresponding scanlines.

## 5 Evaluation

Our evaluation consists of three main parts: First, we illustrate the general difference between a global and a local contrast term. Second, we show the influence of our main model parameters. Last but not least, we demonstrate the quality of our technique with several test image sets and compare to state-of-the-art approaches.

### 5.1 Local Contrast Term

Inspired by Bertalmío et al. [7], let us consider a variational histogram equalisation in Figure 1. In our framework, this can be achieved by setting  $\alpha = 0$  and replacing the simplex constraint (3) by  $0 \leq w(\mathbf{x})f(\mathbf{x}) \leq 1$ . Applying a global contrast term, i.e. degrading  $g_\sigma(\mathbf{x}, \mathbf{y})$  to the constant  $1/|\Omega|$ , yields a standard histogram equalisation (*middle*). On the other hand, a local contrast term allows to visually increase the contrast in the sense of a *Cornsweet illusion* [14] (*right*). This illustrates the general advantages of a local term compared to a global one.

Moreover, we want to point out the following: Our fusion approach is capable of computing weights that produce fusion results with the just discussed Cornsweet illusions. This is very hard to accomplish with standard fusion methods since they do not take into account the quality of the final output image when computing the weights in advance.

### 5.2 Parameters

With this section we illustrate the influence of our model parameters. To this end, we depict several fused images for varying parameter settings in Figure 2.

In the first column, we test the influence of the proposed saturation term. As expected, larger values of  $\beta$  yield more saturated colours. There is a trade-off between a vivid appearance and an unnaturally high amount of colour saturation. In all our experiments, setting  $\beta$  to 1 gives good results. In the second column, different values of  $\mu$  are applied. Since the dispersion term favours solutions that



**Fig. 2.** Influence of model parameters. *From left to right:* Varying  $\beta$  (0 and 2). Larger values of  $\beta$  lead to more saturated colours in the fused image. Varying  $\mu$  (0.1 and 0.9). The larger  $\mu$ , the brighter the fused image. Varying  $\gamma$  (0 and 0.5). The larger  $\gamma$ , the higher the contrast. Varying  $\sigma$  (1% and 100% of image diagonal). The smaller  $\sigma$ , the more local contrast. (Input image source: J. Joffre [3])

**Table 1.** Default parameter setting for all image sets.

$\alpha$	$\beta$	$\gamma$	$\lambda$	$\mu$	$\sigma$
1	1	1/4	0.1	mean of $\bar{f}$	10% of image diagonal

are close to  $\mu$ , it is obvious that larger values lead to brighter results. We propose to determine  $\mu$  automatically as the average over all input images, i.e. the mean of the attachment image  $\bar{f}$ . The third column depicts the composite images for different contrast parameters  $\gamma$ . Choosing it too small yields an image with low contrast, and choosing it too large gives unrealistic appearing images. In general, setting it to 1/4 provides good results. Similar observations apply to the scale parameter  $\sigma$  of the Gaussian in the local contrast term. We observe a larger local contrast with decreasing  $\sigma$ . Also here a trade-off exists: A too large local contrast might be perceived as unnatural. As a rule of thumb, we propose to set  $\sigma$  to 10% of the image diagonal.

In all our experiments below, we apply the discussed procedure to determine  $\mu$  and  $\sigma$  automatically. All other parameters are fixed (cf. Table 1). This allows an easy and straightforward use of our method, even for non-experts. Furthermore, we exploit the complete dynamic range by an affine rescaling of our fused result using the minimal and maximal value of the input stack.

### 5.3 Comparison

Let us now compare our results with competing state-of-the-art exposure fusion methods. In particular, we compare to the method of Kotwal and Chaudhuri [19] (result provided by the authors) and to the popular method of Mertens et al. [23] (code available, executed with recommended parameter setting).



**Fig. 3.** Input images (*first row*) and computed weight maps (*second row*) for an example image set [2]. The brighter the weight map, the larger the weight.



**Fig. 4.** From left to right: Fused images of Kotwal and Chaudhuri [19], Mertens et al. [23], and our result. *Top:* Full images. *Bottom:* Zooms. Particularly at the lamps, the better local contrast provided by our method is obvious.

Figure 3 depicts our computed weight maps for an example input image set with five images. Figure 4 (*right*) shows our corresponding fused composite. Especially in the zooms the higher local contrast of our approach compared to both other methods (*left* and *middle*) is obvious. Moreover, we also observe a colour cast with the method of Kotwal and Chaudhuri. They estimate three individual weights maps for each colour channel. In contrast, our coupled approach that computes joint maps for all channels prevents this colour cast. Additionally, our proposed saturation term provides a vivid colour impression.

To rate the quality of tone mapping operators, Aydin et al. [5] introduced a *Dynamic Range Independent Metric* (DRIM). Based on a model of the human visual system, it measures the distortions between a reference and a test image with different dynamic ranges. We apply this metric here to judge different exposure fusion results. To this end, we use publicly available HDR images [1] as reference, and compute for each HDR image five LDR images separated by one exposure value. These images serve as input for the exposure fusion techniques. Finally, we apply DRIM to compare the reference HDR image with the fused LDR results. DRIM uses the following colour code: Green indicates a loss of visible contrast, blue an amplification of invisible contrast, and red a reversal of visible contrast. In addition, the colour saturation is proportional to the amount

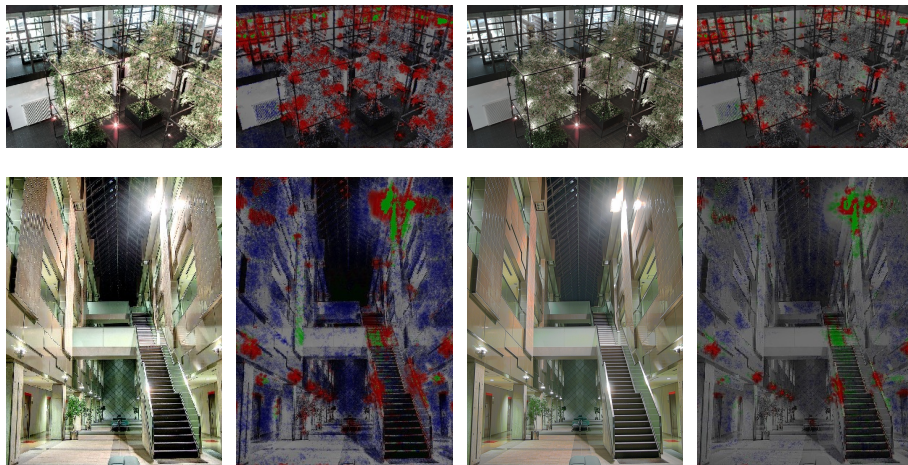


**Fig. 5.** Comparison to exposure fusion of Mertens et al. [23]. *From left to right:* Fused images and DRIM distortion maps of Mertens et al. Fused images and DRIM distortion maps of our method. The more colours, the more distortions.



**Fig. 6.** Fusion of flash and no-flash photographs. *From left to right:* Ambient image, flash image, and our fused result.

of distortion. Figure 5 depicts the fused results and the corresponding DRIM distortion maps for two image sets using the method of Mertens et al. (*left*) and our approach (*right*). It is clearly visible that our results show much less distortions: Especially in the background of the image in the first row, our result contains details that are not visible in the result of Mertens et al. Also our fused composite of the second image set shows less distortions than the one of Mertens et al. Some of the errors in their result are caused by block-like artefacts introduced by the pyramid-based fusion technique. Since we do not apply such a pyramid fusion, our result does not suffer from these distortions.

This evaluation shows that our model produces images with little visible distortions, and thus is well-suited for exposure fusion. To further demonstrate the general applicability of our technique, Figure 7 depicts our fused images for several test data sets. They feature a high amount of visible local contrast, both in dark and bright image regions.

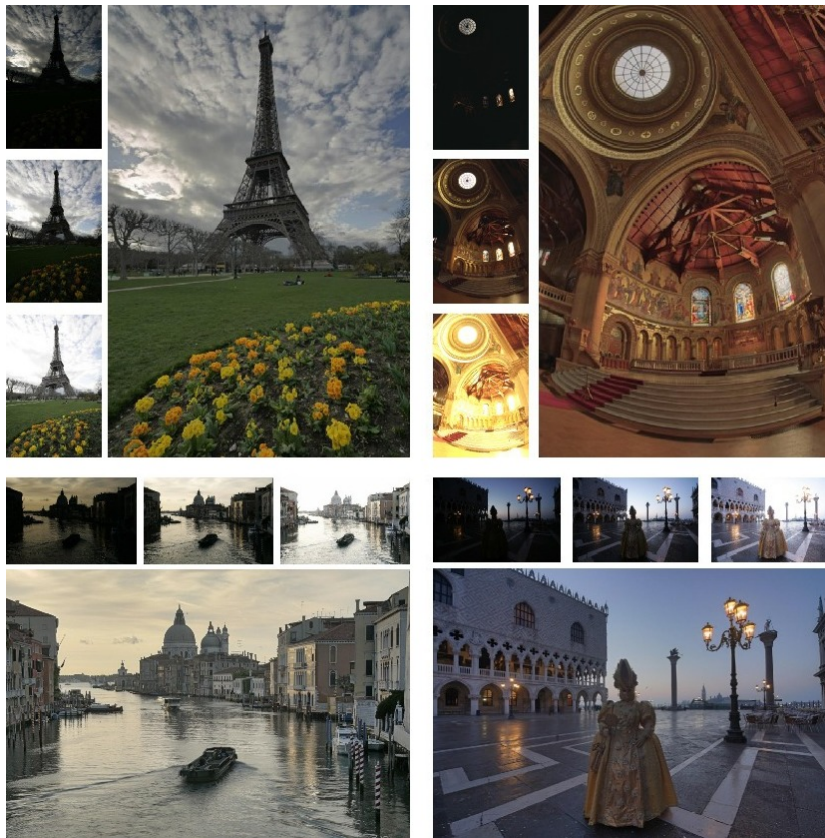


**Fig. 7.** The fusion results for several test image sets demonstrate the high local contrast provided by our method, both in dark and bright image regions. In each case, we show only three representative images of the input set. (Input image sources in reading order: [3], [4], J. Joffre [3], J. Joffre [3])

Besides being independent of the knowledge of the exposure times and the camera response function, our method additionally allows to fuse flash and no-flash photographs. This is illustrated in Figure 6.

## 6 Conclusions and Future Work

We have presented a variational approach for the task of exposure fusion. Our transparent model assumptions implement important perceptually inspired concepts from histogram modification and contrast enhancement. Moreover, all model parameters have an intuitive meaning and can be fixed or determined automatically in a straightforward way. The results of our fusion technique are of high quality and show desirable properties, such as a high local contrast. They compare favourably to state-of-the-art approaches. Moreover, in contrast to the

two-stage procedure of HDR reconstruction and tone mapping, we do not require exposure times or the camera-specific response function. As an additional benefit of that, our approach also shows good results for the fusion of flash and no-flash photographs.

The main concepts of our model are not limited to the fusion of differently exposed images. It might also be applied for all kind of image fusion where features such as a high local contrast are of great importance. Hence, we plan to test and adapt the presented method for other fusion tasks. Moreover, a modification of our approach to unaligned input images is part of future work.

**Acknowledgments.** Our research has been partially funded by the Deutsche Forschungsgemeinschaft (DFG) through a Gottfried Wilhelm Leibniz Prize for Joachim Weickert. This is gratefully acknowledged.

## References

1. [resources.mpi-inf.mpg.de/hdr/gallery.html](http://resources.mpi-inf.mpg.de/hdr/gallery.html)
2. [www.cs.columbia.edu/CAVE/software/rascal/rrslrr.php](http://www.cs.columbia.edu/CAVE/software/rascal/rrslrr.php)
3. [www.hdrsoft.com/examples2.html](http://www.hdrsoft.com/examples2.html)
4. [www.pauldebevec.com/Research/HDR/](http://www.pauldebevec.com/Research/HDR/)
5. Aydin, T.O., Mantiuk, R., Myszkowski, K., Seidel, H.P.: Dynamic range independent image quality assessment. *ACM Transactions on Graphics* 27(3), Article No. 69 (Aug 2008)
6. Bertalmío, M.: From image processing to computational neuroscience: A neural model based on histogram equalization. *Frontiers in Neuroscience* 8, Article No. 71 (Jun 2014)
7. Bertalmío, M., Caselles, V., Provenzi, E., Rizzi, A.: Perceptual color correction through variational techniques. *IEEE Transactions on Image Processing* 16(4), 1058–1072 (Apr 2007)
8. Bertalmío, M., Levine, S.: Variational approach for the fusion of exposure bracketed pairs. *IEEE Transactions on Image Processing* 22(2), 712–723 (Feb 2013)
9. Bertsekas, D.: On the Goldstein-Levitin-Polyak gradient projection method. *IEEE Transactions on Automatic Control* 21(2), 174–184 (Apr 1976)
10. Bogoni, L.: Extending dynamic range of monochrome and color images through fusion. In: *Proc. International Conference on Pattern Recognition*. vol. 3, pp. 7–12. Barcelona, Spain (Sep 2000)
11. Buchsbaum, G.: A spatial processor model for object colour perception. *Journal of the Franklin Institute* 310(1), 1–26 (Jul 1980)
12. Burt, P., Kolczynski, R.: Enhanced image capture through fusion. In: *Proc. International Conference on Computer Vision*. pp. 173–182. Berlin, Germany (May 1993)
13. Cho, W.H., Hong, K.S.: Extending dynamic range of two color images under different exposures. In: *Proc. International Conference on Pattern Recognition*. vol. 4, pp. 853–856. Cambridge, UK (Aug 2004)
14. Cornsweet, T.N.: *Visual Perception*. Harcourt College Publishers, Fort Worth (Jun 1970)
15. Debevec, P.E., Malik, J.: Recovering high dynamic range radiance maps from photographs. In: *Proc. SIGGRAPH 1997*. pp. 369–378. Los Angeles, CA (Aug 1997)

16. Ferradans, S., Bertalmío, M., Provenzi, E., Caselles, V.: An analysis of visual adaptation and contrast perception for tone mapping. *IEEE Transactions on Pattern Analysis and Machine Intelligence* 33(10), 2002–2012 (Oct 2011)
17. Goshtasby, A.A.: Fusion of multi-exposure images. *Image and Vision Computing* 23(6), 611–618 (Jun 2005)
18. Herwig, J., Pauli, J.: An information-theoretic approach to multi-exposure fusion via statistical filtering using local entropy. In: *Proc. International Conference on Signal Processing, Pattern Recognition and Applications*. pp. 50–57. Innsbruck, Austria (Feb 2010)
19. Kotwal, K., Chaudhuri, S.: An optimization-based approach to fusion of multi-exposure, low dynamic range images. In: *Proc. International Conference on Information Fusion*. pp. 1942–1948. Chicago, IL (Jul 2011)
20. Land, E.H., McCann, J.J.: Lightness and retinex theory. *Journal of the Optical Society of America* 61(1), 1–11 (Jan 1971)
21. Mann, S., Picard, R.W.: On being 'undigital' with digital cameras: Extending dynamic range by combining differently exposed pictures. In: *Proc. IS&T Annual Conference*. pp. 442–448. Springfield, VA (May 1995)
22. McCann, J.J.: The role of simple nonlinear operations in modeling human lightness and color sensations. In: Rogowitz, B.E. (ed.) *Human Vision, Visual Processing, and Digital Display*, *Proc. SPIE*, vol. 1077, pp. 355–363. SPIE Press, Bellingham (Aug 1989)
23. Mertens, T., Kautz, J., Van Reeth, F.: Exposure fusion: A simple and practical alternative to high dynamic range photography. *Computer Graphics Forum* 28(1), 161–171 (Mar 2009), [research.edm.uhasselt.be/~tmertens/](http://research.edm.uhasselt.be/~tmertens/)
24. Palma-Amestoy, R., Provenzi, E., Bertalmío, M., Caselles, V.: A perceptually inspired variational framework for color enhancement. *IEEE Transactions on Pattern Analysis and Machine Intelligence* 31(3), 458–474 (Mar 2009)
25. Piella, G.: Image fusion for enhanced visualization: A variational approach. *International Journal of Computer Vision* 83(1), 1–11 (Jun 2009)
26. Raman, S., Chaudhuri, S.: A matte-less, variational approach to automatic scene compositing. In: *Proc. International Conference on Computer Vision*. pp. 574–579. Rio de Janeiro, Brazil (Oct 2007)
27. Raman, S., Chaudhuri, S.: Bilateral filter based compositing for variable exposure photography. In: *Proc. EUROGRAPHICS 2009 (Short Papers)*. pp. 369–378. Munich, Germany (Mar 2009)
28. Reinhard, E., Heidrich, W., Debevec, P., Pattanaik, S., Ward, G., Myszkowski, K.: *High Dynamic Range Imaging: Acquisition, Display, and Image-Based Lighting*. Elsevier, Oxford, 2 edn. (May 2010)
29. Sapiro, G., Caselles, V.: Histogram modification via differential equations. *Journal of Differential Equations* 135(2), 238–268 (Apr 1997)
30. Shalev-Shwartz, S., Singer, Y.: Efficient learning of label ranking by soft projections onto polyhedra. *Journal of Machine Learning Research* 7, 1567–1599 (Jul 2006)
31. Shen, R., Cheng, I., Basu, A.: QoE-based multi-exposure fusion in hierarchical multivariate Gaussian CRF. *IEEE Transactions on Image Processing* 22(6), 2469–2478 (Jun 2013)
32. Shen, R., Cheng, I., Shi, J., Basu, A.: Generalized random walks for fusion of multi-exposure images. *IEEE Transactions on Image Processing* 20(12), 3634–3646 (Dec 2011)
33. Singh, H., Kumar, V., Bhooshan, S.: Weighted least squares based detail enhanced exposure fusion. *ISNR Signal Processing 2014*, Article No. 498762 (Feb 2014)

34. Song, M., Tao, D., Chen, C., Bu, J., Luo, J., Zhang, C.: Probabilistic exposure fusion. *IEEE Transactions on Image Processing* 21(1), 341–357 (Jan 2012)
35. Vavilin, A., Jo, K.H.: Recursive HDR image generation from differently exposed images based on local image properties. In: *Proc. International Conference on Control, Automation and Systems*. pp. 2791–2796. Seoul, Korea (Oct 2008)